Identifying Reactive Intermediates in the Ullmann Coupling Reaction by Scanning Tunneling Microscopy and Spectroscopy†

Meaghan M. Blake, Sanjini U. Nanayakkara,‡ Shelley A. Claridge, Luis C. Fernández-Torres,§ E. Charles H. Sykes,|| and Paul S. Weiss*

Departments of Chemistry and Physics, The Pennsylvania State University, University Park, Pennsylvania 16802-6300

Received: April 19, 2009; Revised Manuscript Received: July 2, 2009

We present an atomic-scale study of substituent effects in the Ullmann coupling reaction on Cu{111} using low-temperature scanning tunneling microscopy and spectroscopy. We have observed fluorophenyl intermediates and phenyl intermediates as well as biphenyl products on Cu{111} after exposure to 4-fluoro-1-bromobenzene (p-FC_6H_4Br) and bromobenzene (C_6H_5Br), respectively. When p-FC_6H_4Br dissociatively chemisorbs at 298 K on Cu{111}, the relatively weakly bound Br dissociates, and fluorophenyl intermediates are formed. These intermediates couple to form 4,4′-difluorobiphenyl and desorb at temperatures below 370 K. However, by cooling the substrate to low temperature (4 K), we have observed unreacted fluorophenyl intermediates distributed randomly on terraces and at step edges of the Cu{111} surface. Alternatively, at similar coverages of C_6H_5Br, we have observed biphenyl distributed on terraces and step edges. In each case, Br adatoms were randomly distributed on the surface. Chemical identification of fluorophenyl and phenyl intermediates and biphenyl products was achieved by vibrational spectroscopy via inelastic tunneling spectroscopy. The strongest vibrational mode in the phenyl species disappears when the tilted intermediates couple to form biphenyl products. We infer that the surface normal component of the dipole moment is important in determining the transition strength in inelastic electron tunneling spectroscopy.

Introduction

Tunneling spectroscopy is a powerful technique that enables the identification of surface adsorbates and provides insight into the bonding and chemical environment of molecules on surfaces.[1−8] Tunneling spectroscopy of molecular vibrations was first demonstrated by Jaklevic and Lambe in 1966.[7,8] Using a thin-film metal−oxide−metal tunneling junction, they were able to observe vibrational energies of molecules contained within the junction. They found that sharp increases in the tunneling conductance could be observed when the energy of the tunneling electrons reached the energy of a vibrational mode of the molecules. Such changes in conductance occur when tunneling electrons inelastically transfer their energy to vibrational modes, giving rise to an inelastic tunneling channel.[1] Measurement of these vibrational modes is referred to as inelastic electron tunneling spectroscopy (IETS).

Later, Gregory used crossed wires separated by a monolayer of adsorbed molecules to perform IETS.[9] Two peaks were observed, 173 and 359 mV, which were consistent with the C−H stretching and bending vibrations of hydrocarbon contaminants in the junction. Most significantly, this demonstrated that IETS was possible in a microscopic tunneling junction.

More recently, the capabilities of IETS have been extended by using the junction of a scanning tunneling microscope (STM) to probe vibrational modes at the single-molecule level.[1−5] Such spectroscopies were anticipated early after the invention of the STM.[10−17] In contrast with metal−oxide−metal junctions, where molecules are randomly oriented at rough interfaces and all possible modes are observed,[18,19] selection rules are expected to limit the allowed tunneling transitions for individual molecules. Ho and coworkers demonstrated the ability of IETS to distinguish between isotopically substituted molecules on surfaces[1,3] and between molecules adsorbed on surfaces through different bonding geometries.[2]

Previously, we observed low-energy adsorbate−substrate vibrational modes of benzene molecules on a Ag{110} surface.[5] We found that the energies of vibrational modes vary depending on the adsorption site, demonstrating that tunneling spectroscopy is sensitive to the chemical environment. We have also utilized IETS to probe the vibrational modes of hydrogen atoms on Pd{111}.[4] We and others have found that the vibrational modes are related to the barriers to motion, providing insight into the magnitude of these barriers and the mechanisms by which adsorbates become mobile on the surface at low temperatures.

Scanning tunneling spectroscopy (STS) with the STM can provide key insight into surface reactions on the molecular scale. In most previous studies, the reactants and products have been imaged exclusively.[20−25] However, probing isolated reactive intermediates can provide important details of reaction mechanisms and dynamics on surfaces.[25−30] Here we present a low-temperature atomic-scale study of substituent effects in the Ullmann coupling reaction on Cu{111} using STM and STS. We have used STS to infer the adsorption geometry of the reactive intermediates and have successfully identified the unreacted/reacted status of the intermediates.

Ullmann coupling is an organic reaction of two haloaromatics to form a biaromatic molecule via a copper catalyst.[31] Using temperature-programmed desorption (TPD), Bent and coworkers

† Part of the "Robert W. Field Festschrift".

* Corresponding author. E-mail: stm@psu.edu.

‡ Current address: Materials Science and Engineering Department, University of Pennsylvania, Philadelphia, PA 19104.

§ Current address: Department of Chemistry, University of Puerto Rico at Cayey, Cayey, Puerto Rico 00736.

|| Current address: Department of Chemistry, Tufts University, Medford, MA 02155.

10.1021/jp903590c CCC: $40.75
Published on Web 08/06/2009

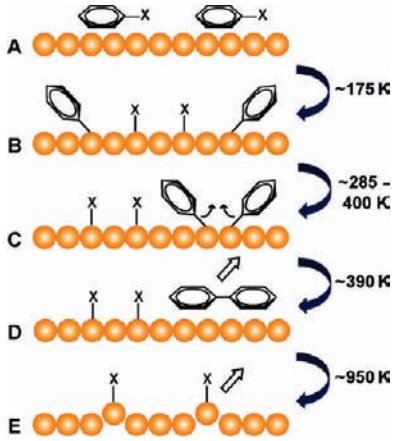

Figure 1. Schematic of the Ullmann coupling reaction. (A) Aromatic halides adsorb onto the Cu{111} catalyst. (B) Adsorbed phenyl intermediates and halide adatoms are formed on Cu{111} via dissociative chemisorption at ~175 K. (C) Subsequent recombination of pairs of phenyl intermediates forms biphenyl at ~285−400 K, depending on the coverage of the aromatic halide. (D) Desorption of biphenyl occurs at ~390 K, whereas (E) halide adatoms desorb as CuX at ~950 K.

found that the reaction between two iodobenzene (C_6H_5I) molecules to form biphenyl takes place on Cu{111} with 100% selectivity.[32] A schematic of the Ullmann coupling reaction on Cu{111} is shown in Figure 1. They found that the temperature at which biphenyl is formed depends on the surface coverage of the haloaromatic. At submonolayer coverage, C_6H_5I dissociates to form phenyl intermediates and iodine adatoms at 175 K. At 370 K, the phenyl intermediates are mobile and couple to form biphenyl.[32] Therefore, at low surface coverage, only phenyl intermediates are observed, as confirmed by STM.[27] As the surface coverage increases, a desorption peak for biphenyl can be observed at ~285 K in TPD data, suggesting that at higher surface exposure of the haloaromatic, biphenyl would be observed. Bent and coworkers recorded the vibrational spectra of the tilted phenyl intermediates using high-resolution electron energy loss spectroscopy (HREELS).[33]

Previously, Rieder and coworkers demonstrated that the STM tip can be used to induce the steps of the Ullmann coupling reaction, even at low temperature (20 K).[34] After dissociative chemisorption of C_6H_5I to form phenyl intermediates and iodine, they manipulated phenyl intermediates at the step edges into proximity. Using voltage pulses applied by the STM tip, they rotated and coupled the intermediates to form biphenyl.[34]

We have previously observed protopolymer chains as a result of dissociative chemisorption of 1,4-diiodobenzene on Cu{111}.[29] We found that the incident reactant molecule dissociatively chemisorbed to form a phenylene intermediate and two iodine adatoms.[28,29] The phenylene intermediates subsequently self-assembled into chains through substrate-mediated and intermolecular interactions. We confirmed these noncovalent interactions using molecular manipulation with the STM tip at low temperatures.

Most recently, Rosei and coworkers formed polyphenylene molecular wires with the Ullmann coupling reaction using 1,4-diiodobenzene and 1,3-diiodobenzene.[30] These molecules dissociatively chemisorbed after they were deposited onto a Cu{110} surface, forming phenylene intermediates. Subsequent annealing resulted in the formation of linear and zigzag chains, respectively.

Here we have used both STM and STS to study Cu{111} after exposure to both bromobenzene (C_6H_5Br) and 4-fluoro-1-bromobenzene (p-FC_6H_4Br). We observed biphenyl as a result of depositing C_6H_5Br but observed only uncoupled fluorophenyl intermediates when using p-FC_6H_4Br at the same surface coverages. These species have different spectroscopic signatures, enabling us to distinguish between the reactive intermediates and the products of the Ullmann coupling reaction.

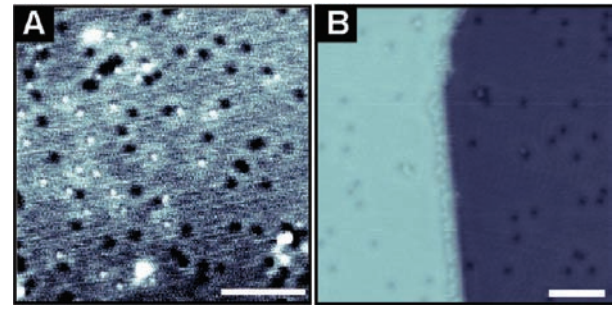

Figure 2. Scanning tunneling microscopy images of Cu{111} after a 200 L exposure to p-FC_6H_4Br. Fluorophenyl intermediates (protrusions) and Br adatoms (depressions) were found scattered along step edges and randomly distributed among terraces. (A) $I_t = 40$ pA, $V_s = -0.3$ V. (B) $I_t = 30$ pA, $V_s = -0.3$ V. The scale bar in A is 100 Å and the scale bar in B is 50 Å.

Experiments

Experiments were performed in a custom-built ultrastable cryogenic extreme-high vacuum STM, described elsewhere.[35] In brief, the Cu{111} single crystal (MaTecK, Jülich, Germany) was cleaned by 1 keV Ar^+ bombardment followed by annealing at ~850 K. p-FC_6H_4Br (99% Aldrich) and C_6H_5Br were purified by freeze−pump−thaw cycles and deposited via a high-precision sapphire leak valve. The purity of the molecules was verified in situ by residual gas analysis using a quadrupole mass spectrometer. We exposed the clean Cu{111} single crystal to the molecule of interest (p-FC_6H_4Br or C_6H_5Br) by backfilling the main chamber with vapor at room temperature. Exposures are hereafter reported in Langmuirs ($1\ L = 1 \times 10^{-6}$ Torr·s). Ion gauges and ion pumps were turned off in the main chamber during exposure to minimize molecular fragmentation prior to adsorption. Following exposure, the substrate was immediately transferred to the STM held at 4 K.

All STM images were acquired in constant-current mode at 4 K. Tunneling spectra were recorded under open feedback conditions in differential conductance (dI/dV) mode using a lock-in amplifier (Stanford Research Systems, model SR850, Sunnyvale, CA). In dI/dV mode, we measured the first harmonic of the tunneling current by superimposing a 1 kHz ($V_{rms} = 16$ mV) AC modulation onto the bias signal.

Because d^2I/dV^2 data were not directly acquired, vibrational modes were extracted from dI/dV spectra through numerical differentiation. We reduced noise in the spectra by processing with Matlab data analysis software (Matlab version R2007a, The Mathworks, Natick, MA) using a sliding window convolution filter with a window length of 50 mV. Taking the numerical derivative yielded d^2I/dV^2, which was also smoothed using a sliding window convolution filter with a window length of 60 mV.

Results and Discussion

Typical scanning tunneling microscopy images of Cu{111} after a 200 L dose of p-FC_6H_4Br are shown in Figure 2. Both protrusions (distributed along step edges and on terraces) and depressions (randomly distributed on terraces) were observed.

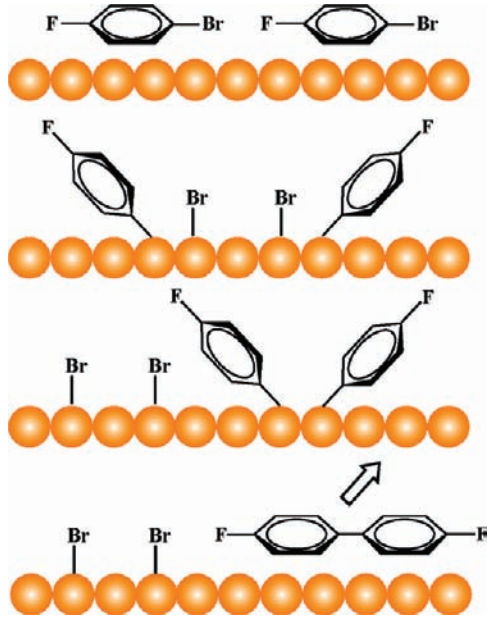

Figure 3. Schematic of the proposed mechanism for the Ullmann coupling reaction between two *p*-FC_6H_4Br molecules that couple to form a symmetric dihalogenated-biphenyl molecule on Cu{111}. As discussed in the text, only the C−Br bonds dissociate.

Line scan measurements taken over the apparent protrusions gave an average length of 3.4 ± 0.8 Å. (Details are provided in the Supporting Information.) The depressions were assigned as Br adatoms, and the protrusions were assigned as fluorophenyl intermediates. These assignments were confirmed with spectroscopic measurements and are discussed below. We and others have previously identified halogen atoms on Cu{111}.[27,28,36] The placement of the Br adatoms was consistent with marking the sites at which dissociative chemisorption took place.[28]

A schematic of the expected reaction pathway of *p*-FC_6H_4Br on Cu{111} is shown in Figure 3. On the basis of the previous TPD and STM results,[27,32,33] we expect *p*-FC_6H_4Br to chemisorb dissociatively on Cu{111} at 298 K to form fluorophenyl intermediates and Br adatoms. Because the bond enthalpies of C−Br and C−F of C_6H_5X (X = Br, F) are 351 and 531 kJ/mol, respectively,[37] we expect only the C−Br bond to dissociate upon adsorption. Also, it has been shown by TPD experiments using fluoroiodobenzene (*p*-FC_6H_4I) that fluorination of a haloaromatic influences only reaction kinetics, not its mode of interaction with the surface.[38]

We find that only one C−X (X = Br, F) bond dissociates upon adsorption of *p*-FC_6H_4Br on Cu{111} at 298 K, which we have assigned as C−Br. Previously, we and others have shown that *p*-diiodobenzene ($C_6H_4I_2$) dissociates on Cu{111} at 298 K to produce phenylene intermediates by dissociation of both C−I bonds and that these phenyl moieties align to form molecular chains on the surface.[26,29,30] Because we did not observe molecular chains, we conclude that only one of the C−X bonds dissociated upon adsorption of *p*-FC_6H_4Br to form halogenated-phenyl intermediates. Additionally, IR vibrational spectra of halogen-substituted fluorobenzene molecules have shown that the bending and stretching frequencies of the C−F bond remain unchanged regardless of substitution pattern,[39] suggesting similar C−F bond enthalpies for *p*-FC_6H_4Br and C_6H_5F. Therefore, we conclude that because C−Br is the weaker bond, it dissociates upon adsorption.

Fluorine substitution is expected to change the temperature at which phenyl intermediates couple. Gellman and coworkers derived the linear free energy relationship (Hammet plot) for the Ullmann coupling reaction by TPD experiments using iodobenzene (C_6H_5I) and iodobenzene derivatives (*p*-FC_6H_4I, *m*-FC_6H_4I, *o*-FC_6H_4I, *m*-$CH_3C_6H_4I$).[38] The slope of the Hammet plot indicates that the transition state of the Ullmann coupling reaction is electron rich with respect to the initial state. Therefore, the placement of fluorine, an electron-withdrawing substituent, at the para position of C_6H_5I would stabilize the transition state, lowering the energy barrier to coupling. Fluorine substitution also increases repulsion between molecules at high coverages, which leads to a decrease in the energy barrier to desorption.[33] Therefore, we expected fluorophenyl intermediates to couple to form 4,4′-difluorobiphenyl and to desorb from the surface at lower temperatures than the unsubstituted molecules because of these stronger repulsive forces.

To test our assignment of the protrusions as fluorophenyl intermediates, we acquired tunneling spectra (d*I*/d*V*) over the bare Cu surface and the apparent protrusions (tentatively assigned as fluorophenyl) and depressions (consistent with previous STM observations of Br on Cu{111}; under some tunneling conditions, the Br adatoms appeared to have a sombrero-like shape in STM images, a central peak surrounded by a depressed ring, also consistent with prior observations, as seen in Figure 4A. Tunneling spectra of bare Cu (Figure 4B) show the surface state at 430 meV below the Fermi level, which is characteristic of Cu{111}. However, this surface state is absent over the depression (Figure 4D), as seen in our earlier data.[36] Halogens are known to quench the surface state of Cu{111},[36,40] although this observation does not differentiate between the two possible surface-bound halogens on Cu{111}.

The d*I*/d*V* spectra acquired over fluorophenyl (C, the apparent protrusion in Figure 4A) show sharp increases in conductance at −110 and +86 meV. On the basis of HREELS measurements of phenyl on Cu{111}, 90 meV corresponds to a C−H out-of-plane bending mode that is a result of the bonding geometry of phenyl on Cu{111}.[33,41] This feature dominates HREELS spectra. Near-edge X-ray absorption fine structure (NEXAFS) measurements indicate that the adsorbed phenyl is tilted significantly away from the surface plane by an angle of ∼43°.[32,41] Selection rules for active vibrational modes in tunneling spectroscopy are not well understood, and not all observed modes in traditional vibrational techniques (e.g., IR, HREELS) are observed in inelastic tunneling spectra.[1,3,5,20,42−44] Importantly, in IETS, we observe modes in which there is a significant contribution to the surface normal component of the dipole moment.

Vibrational modes of adsorbed molecules can be identified using the second derivative of conductance (d^2I/dV^2). Although this signal is often acquired directly, here we extracted this information from the d*I*/d*V* spectra through numerical differentiation. Figure 5 shows an analysis of both a single spectrum (Figure 5A) taken over a presumed fluorophenyl intermediate from the STM image in Figure 4 and a set of averaged data taken from six sequential d*I*/d*V* scans of the same adsorbate (Figure 5B). We reduced noise in the d*I*/d*V* spectra (green traces) by processing with Matlab data analysis software (Matlab version R2007a, The Mathworks, Natick, MA) using a sliding window convolution filter with a window length of 50 mV. The numerical derivative yielded d^2I/dV^2 (blue traces), which was also smoothed with a 60 mV window convolution (dark blue traces) to facilitate peak assignments.

Individual and averaged d^2I/dV^2 traces exhibit strong peaks at −110 and +86 meV and at −94 and +97 meV, respectively, which is in reasonable agreement with the dominant, strong

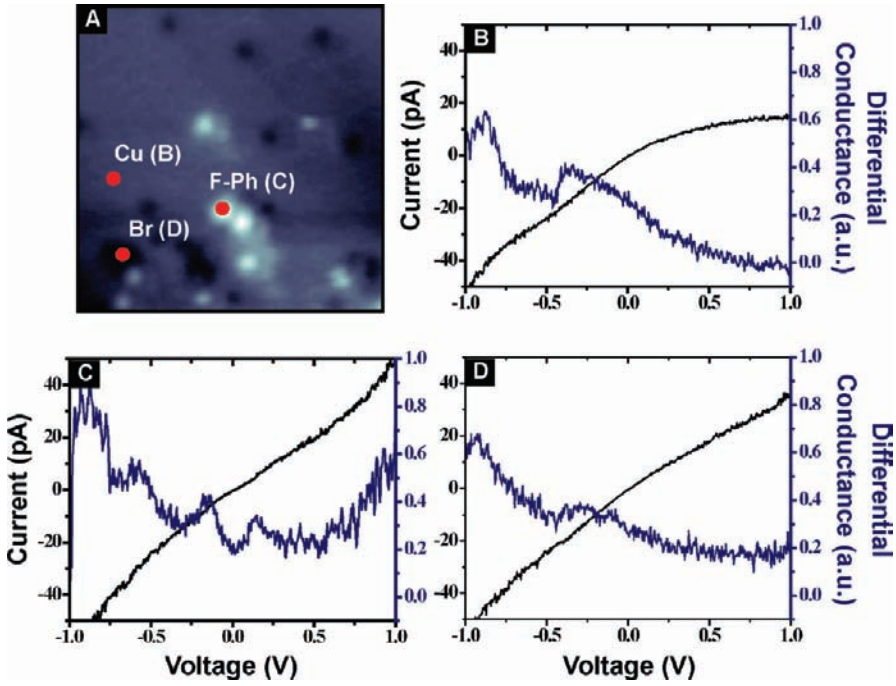

Figure 4. (A) Scanning tunneling microscopy image (145 Å × 145 Å, $I_t = 40$ pA, $V_s = -0.75$ V) of Cu{111} after a 200 L exposure to p-FC_6H_4Br and corresponding tunneling spectra acquired over: (B) the bare Cu surface, (C) a protrusion (in close proximity to another), assigned as a fluorophenyl intermediate, and (D) a Br adatom, are shown.

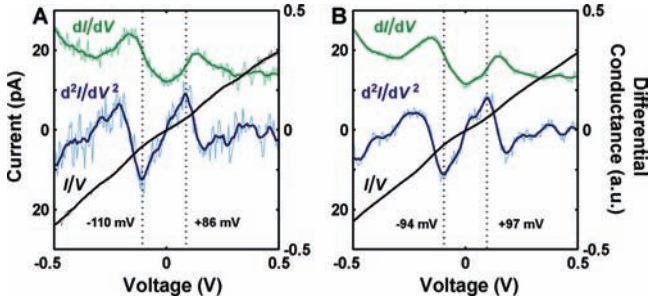

Figure 5. Analysis of (A) a single spectrum taken over a fluorophenyl intermediate from the STM image in Figure 4, and (B) a set of averaged data taken from six sequential dI/dV sweeps over the same adsorbate. Noise was reduced in the dI/dV spectra (green) using a sliding window convolution filter, as described in the text. The numerical derivative yielded d^2I/dV^2 (light blue), which was also smoothed (dark blue) to facilitate peak analysis.

C−H out-of-plane vibrational mode (90 meV) observed in HREELS studies of phenyl adsorbates on Cu{111}.[33] Peaks from weak vibrational modes (ring stretch, C−H in-plane bend, and others) evident as shoulders or very weak peaks in HREELS, were not observed here presumably because of peak broadening and low signal-to-noise. It should be noted that although the HREELS studies mentioned above refer to vibrational modes of unsubstituted phenyl adsorbates, previous IR studies of benzene and fluorobenzene indicate that fluorination does not impact C−H bending and stretching modes.[39] Importantly, this mode would be expected to have greatly reduced intensity in biphenyl, which is bound parallel to the surface, consistent with the dipole selection rules discussed above. Therefore, on the basis of the identification of the C−H out-of-plane bending mode, we identify the adsorbate as a fluorophenyl intermediate.

In our system, differences in adsorbate characteristics near step edges could be expected to lead to different desorption temperatures of reaction products. Therefore, we acquired STS over fluorophenyl intermediates adsorbed at step edges, as shown in Figure 6. These adsorbates did not display the same spectroscopic signatures as molecules adsorbed on terraces. We infer that this may be due to the fluorophenyl intermediates bound to step edges adsorbed at different angles than those on terraces.[32,33] This result requires further study to elucidate the roles of step edges in surface chemical reactions.[45−58]

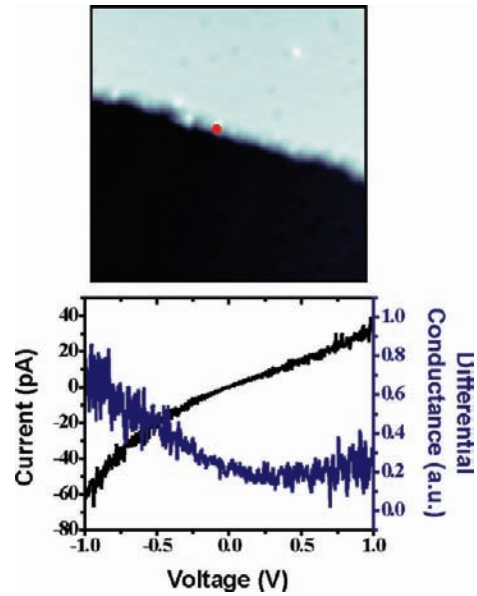

Figure 6. Scanning tunneling microscopy image and corresponding tunneling spectrum acquired over a fluorophenyl intermediate adsorbed at a surface step edge (150 Å × 150 Å; $I_t = 50$ pA; $V_s = -0.75$ V). Both the conductance (black) and differential conductance (blue) spectra are shown. The fluorophenyl intermediates bound at step edges did not display the same spectroscopic signatures as those adsorbed on terraces.

To test our assignment of fluorophenyl intermediates, we exposed clean Cu{111} to 200 L of C_6H_5Br. On the basis of TPD data mentioned previously,[32] we expected to see biphenyl molecules at high coverage because there was only one

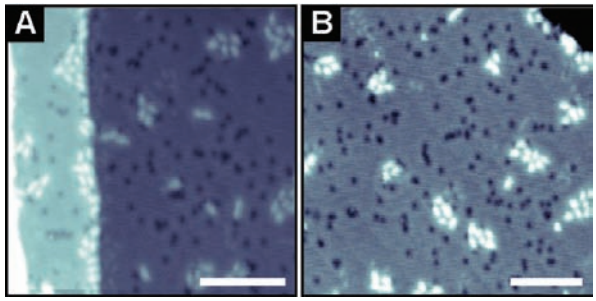

Figure 7. Scanning tunneling microscopy images of Cu{111} after a 200 L exposure to C_6H_5Br showing molecules along the entire length of the step edge and grouped on terraces. Depressions can also be observed. (A) $I_t = 22$ pA, $V_s = -0.75$ V. (B) $I_t = 17$ pA, $V_s = -0.75$ V. The scale bar in each image is 100 Å.

substituent group. Scanning tunneling microscopy images of this surface after exposure are shown in Figure 7. Again, two surface-bound species are observed in STM images: apparent protrusions, oblong in shape (in contrast to the shape of phenyl intermediates), distributed along terraces and step edges, and apparent depressions, which were randomly distributed on terraces. Line scan measurements taken over the apparent protrusions gave an average protrusion length of 8.7 ± 2.1 Å as compared with the model length for biphenyl of 6.9 Å. (See the Supporting Information.) Because protrusions in STM images arise from a convolution of topographic and electronic structure,[59] protrusion lengths are typically measured as the peak width at a fixed percentage of the peak maximum value; here we use a threshold of 85% (details provided in the Supporting Information), which is expected to be somewhat larger than the model values (as defined). In contrast with biphenyl, line scans of adjacent uncoupled phenyl intermediates typically have a local topographic minimum between them.[27] Therefore, we assign the apparent protrusions as biphenyl and the apparent depressions or sombrero-shaped features as Br adatoms, consistent with our and others' prior results on Cu{111}.[34,36]

Spectroscopic measurements were acquired over the apparent protrusions and depressions and the bare Cu surface (Figure 8). The apparent depressions showed quenching of the surface state of Cu{111}, similar to that in Figure 4D, which is consistent with identification as Br adatoms (Figure 8B). In the spectra acquired over the protrusions, no strong features were observed above our noise level, unlike the differential conductance measurements for the fluorophenyl intermediates (Figure 8A). This is consistent with the orientation of biphenyl lying flat on Cu{111} with its conjugated π system parallel to the surface.[33] These measurements are in agreement with our earlier measurements being due to tilted fluorophenyl intermediates and not to 4,4′-difluorobiphenyl molecules.

Conclusions

We have shown that at high coverage of p-FC_6H_4Br on Cu{111}, only fluorophenyl intermediates and halogen adatoms are observed on the surface. We verified this observation by assigning vibrational modes from differentiated IETS. Because fluorination of the ring in the para position stabilizes the transition state and lowers the barrier to coupling and desorption, only intermediates were observed. The vibrational modes were assigned on the basis of previous HREELS experiments and correspond to the tilted bonding geometry of phenyl and related species. We find that selection rules for IETS require dipole components normal to the surface to be observed. If the

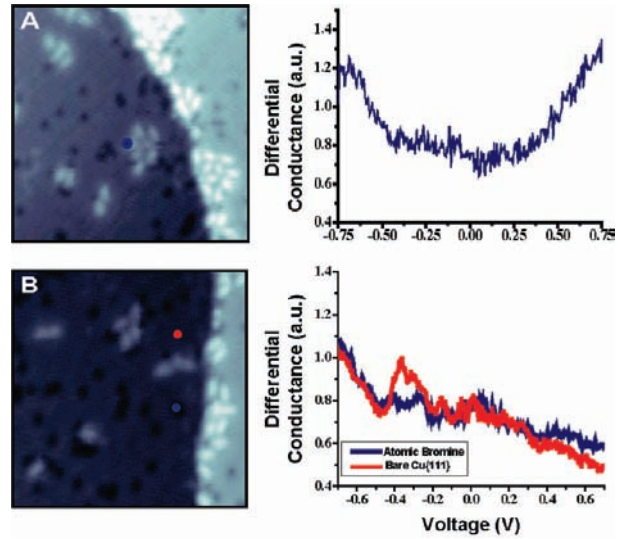

Figure 8. Scanning tunneling microscopy images of Cu{111} after a 200 L exposure to C_6H_5Br and corresponding tunneling spectra are shown. Differential conductance spectra acquired over: (A) a biphenyl molecule, indicated by the blue circle on the STM image (220 Å × 220 Å, $I_t = 20$ pA, $V_s = -0.75$ V) and (B) the bare Cu{111} surface (red) and Br adatoms (blue) (220 Å × 220 Å, $I_t = 20$ pA, $V_s = -0.75$ V). Note that the surface state of Cu{111} at −43 meV is quenched locally by the bromine adatoms.

fluorophenyl intermediates were adsorbed parallel to the surface, we would not expect to have observed any strong vibrational modes. We compared these findings to STS acquired over biphenyl molecules after exposing Cu{111} to C_6H_5Br, which appeared featureless under our experimental conditions because of the orientation of biphenyl with its rings parallel to the surface.

Acknowledgment. We gratefully acknowledge financial support from the National Science Foundation and the Office of Naval Research. Additionally, we thank Patrick Han and Adam Kurland for helpful discussions. This article is dedicated to Bob Field, a mentor and friend who has had tremendous impact on our thinking and our approach to science.

Supporting Information Available: Details of the calculations of apparent molecular length and model lengths for fluorophenyl and biphenyl. This material is available free of charge via the Internet at http://pubs.acs.org.

References and Notes

(1) Stipe, B. C.; Rezaei, M. A.; Ho, W. *Science* **1998**, *280*, 1732.
(2) Lauhon, L. J.; Ho, W. *J. Phys. Chem. A* **2000**, *104*, 2463.
(3) Lauhon, L. J.; Ho, W. *Phys. Rev. B* **1999**, *60*, R8525.
(4) Fernandez-Torres, L. C.; Sykes, E. C. H.; Nanayakkara, S. U.; Weiss, P. S. *J. Phys. Chem. B* **2006**, *110*, 7380.
(5) Pascual, J. I.; Jackiw, J. J.; Song, Z.; Weiss, P. S.; Conrad, H.; Rust, H.-P. *Phys. Rev. Lett.* **2001**, *86*, 1050.
(6) Bartels, L.; Meyer, G.; Rieder, K. H. *Chem. Phys. Lett.* **1998**, *297*, 287.
(7) Jaklevic, R. C.; Lambe, J. *Phys. Rev. Lett.* **1966**, *17*, 1139.
(8) Lambe, J.; Jaklevic, R. C. *Phys. Rev.* **1968**, *165*, 821.
(9) Gregory, S. *Phys. Rev. Lett.* **1990**, *64*, 689.
(10) Binnig, G.; Garcia, N.; Rohrer, H. *Phys. Rev. B* **1985**, *32*, 1336.
(11) Persson, B. N. J.; Baratoff, A. *Phys. Rev. Lett.* **1987**, *59*, 339.
(12) Persson, B. N. J.; Demuth, J. E. *Solid State Commun.* **1986**, *57*, 769.
(13) Hamers, R. J.; Demuth, J. E. *Phys. Rev. Lett.* **1988**, *60*, 2527.
(14) van Loenen, E. J.; Demuth, J. E.; Tromp, R. M.; Hamers, R. J. *Phys. Rev. Lett.* **1987**, *58*, 373.
(15) Baratoff, A.; Persson, B. N. J. *J. Vac. Sci. Technol., A* **1988**, *6*, 331.

(16) Feenstra, R. M. *Surf. Sci.* **1994**, *299/300*, 965.
(17) Smith, D. P. E.; Kirk, M. D.; Quate, C. F. *J. Chem. Phys.* **1987**, *86*, 6034.
(18) Hansma, P. K. *Tunneling Spectroscopy*; Plenum Press: New York, 1982.
(19) Wolfram, T. *Inelastic Electron Tunneling Spectroscopy*; Springer-Verlag: Berlin, 1978.
(20) Lee, H. J.; Ho, W. *Science* **1999**, *286*, 1719.
(21) Sprunger, P. T.; Okawa, Y.; Besenbacher, F.; Stensgaard, I.; Tanaka, K. *Surf. Sci.* **1995**, *344*, 98.
(22) Schroder, U.; McIntyre, B. J.; Salmeron, M.; Somorjai, G. A. *Surf. Sci.* **1995**, *331*, 337.
(23) Okawa, Y.; Tanaka, K. *Surf. Sci.* **1995**, *344*, L1207.
(24) McIntyre, B. J.; Salmeron, M.; Somorjai, G. A. *Science* **1994**, *265*, 1415.
(25) Weigelt, S.; Bombis, C.; Busse, C.; Knudsen, M. M.; Gothelf, K. V.; Laegsgaard, E.; Besenbacher, F.; Linderoth, T. R. *ACS Nano* **2008**, *2*, 651.
(26) Sykes, E. C. H.; Han, P.; Kandel, S. A.; Kelly, K. F.; McCarty, G. S.; Weiss, P. S. *Acc. Chem. Res.* **2003**, *36*, 945.
(27) Weiss, P. S.; Kamma, M. M.; Graham, T. M.; Stranick, S. J. *Langmuir* **1998**, *14*, 1284.
(28) McCarty, G. S.; Weiss, P. S. *J. Phys. Chem. B* **2002**, *106*, 8005.
(29) McCarty, G. S.; Weiss, P. S. *J. Am. Chem. Soc.* **2004**, *126*, 16772.
(30) Lipton-Duffin, J. A.; Ivasenko, O.; Perepichka, D. F.; Rosei, F. *Small* **2009**, *5*, 592.
(31) Ullmann, F.; Meyer, G.; Loewenthal, O.; Gilli, E. *Justus Liebigs Ann. Chem.* **1904**, *332*, 38.
(32) Xi, M.; Bent, B. E. *J. Am. Chem. Soc.* **1993**, *115*, 7426.
(33) Xi, M.; Bent, B. E. *Surf. Sci.* **1992**, *278*, 19.
(34) Hla, S. W.; Bartels, L.; Meyer, G.; Rieder, K. H. *Phys. Rev. Lett.* **2000**, *85*, 2777.
(35) Stranick, S. J.; Kamna, M. M.; Weiss, P. S. *Rev. Sci. Instrum.* **1994**, *65*, 3211.
(36) Nanayakkara, S. U.; Sykes, E. C. H.; Fernandez-Torres, L. C.; Blake, M. M.; Weiss, P. S. *Phys. Rev. Lett.* **2007**, 98.
(37) Blanksby, S. J.; Ellison, G. B. *Acc. Chem. Res.* **2003**, *36*, 255.
(38) Meyers, J. M.; Gellman, A. J. *Surf. Sci.* **1995**, *337*, 40.
(39) Narasimham, N. A.; Elsabban, M. Z.; Nielsen, J. R. *J. Chem. Phys.* **1956**, *24*, 420.
(40) Turton, S.; Kadodwala, M.; Jones, R. G. *Surf. Sci.* **1999**, *442*, 517.
(41) Yang, M. X.; Xi, M.; Yuan, H. J.; Bent, B. E.; Stevens, P.; White, J. M. *Surf. Sci.* **1995**, *341*, 9.
(42) Sainoo, Y.; Kim, Y.; Okawa, T.; Komeda, T.; Shigekawa, H.; Kawai, M. *Phys. Rev. Lett.* **2005**, 95.
(43) Moresco, F.; Meyer, G.; Rieder, K. H. *Mod. Phys. Lett. B* **1999**, *13*, 709.
(44) Hipps, K. W.; Mazur, U. *J. Phys. Chem.* **1993**, *97*, 7803.
(45) Kamna, M. M.; Stranick, S. J.; Weiss, P. S. *Science* **1996**, *274*, 118.
(46) Stranick, S. J.; Kamna, M. M.; Weiss, P. S. *Science* **1994**, *266*, 99.
(47) Sykes, E. C. H.; Han, P.; Weiss, P. S. *J. Phys. Chem. B* **2003**, *107*, 5016.
(48) Yoon, H. A.; Salmeron, M.; Somorjai, G. A. *Surf. Sci.* **1997**, *373*, 300.
(49) Zambelli, T.; Wintterlin, J.; Trost, J.; Ertl, G. *Science* **1996**, *273*, 1688.
(50) Dahl, S.; Logadottir, A.; Egeberg, R. C.; Larsen, J. H.; Chorkendorff, I.; Tornqvist, E.; Norskov, J. K. *Phys. Rev. Lett.* **1999**, *83*, 1814.
(51) Liu, Z. P.; Hu, P. *J. Am. Chem. Soc.* **2003**, *125*, 1958.
(52) Zubkov, T.; Morgan, G. A.; Yates, J. T.; Kuhlert, O.; Lisowski, M.; Schillinger, R.; Fick, D.; Jansch, H. J. *Surf. Sci.* **2003**, *526*, 57.
(53) Vang, R. T.; Honkala, K.; Dahl, S.; Vestergaard, E. K.; Schnadt, J.; Laegsgaard, E.; Clausen, B. S.; Norskov, J. K.; Besenbacher, F. *Surf. Sci.* **2006**, *600*, 66.
(54) Vang, R. T.; Honkala, K.; Dahl, S.; Vestergaard, E. K.; Schnadt, J.; Laegsgaard, E.; Clausen, B. S.; Norskov, J. K.; Besenbacher, F. *Nat. Mater.* **2005**, *4*, 160.
(55) Gambardella, P.; Sljivancanin, Z.; Hammer, B.; Blanc, M.; Kuhnke, K.; Kern, K. *Phys. Rev. Lett.* **2001**, 87.
(56) Crommie, M. F.; Lutz, C. P.; Eigler, D. M. *Nature* **1993**, *363*, 524.
(57) Avouris, P.; Lyo, I.-W.; Molinas-Mata, P. *Chem. Phys. Lett.* **1995**, *240*, 423.
(58) Hasegawa, Y.; Avouris, P. *Phys. Rev. Lett.* **1993**, *71*, 1071.
(59) Eigler, D. M.; Weiss, P. S.; Schweizer, E. K.; Lang, N. D. *Phys. Rev. Lett.* **1991**, *66*, 1189.

JP903590C